Electronic charge distribution in silicon

Moshe Deutsch* and Michael Hart
Wheatstone Laboratory, King's College, Strand, London WC2R 2LS, England
(Received 4 April 1984; revised manuscript received 29 August 1984)

The structure factors F_h of eight high-order [$0.64 \leq (\sin\theta)/\lambda \leq 1.56$ Å^{-1}] reflections were measured for a number of wavelengths to an accuracy of a few thousandths of an electron per atom. Most of these have never been measured before to this level of accuracy. A monolithic double-crystal diffractometer of novel design was employed in measuring thin-crystal Laue-case rocking curves which exhibit fine structure strongly dependent on F_h. Computer fitting of the theoretical curve to the measured one yields F_h. An energy-dispersive mode of operation allowed simultaneous measurements of the rocking curves of a whole family of planes to be carried out. The F_h values obtained, while in excellent agreement with previously measured and theoretical ones for $(\sin\theta)/\lambda < 1$ Å^{-1}, are consistently and increasingly lower than the theoretical relativistic Hartree-Fock F_h values for $(\sin\theta)/\lambda > 1$ Å^{-1}. This systematic trend most probably reflects the inadequacy of the Debye parameter B calculated from medium- and low-order F_h's for high-order reflections. Assuming different vibrational amplitudes for intermediate- and inner-shell electrons, our data yield $B_{\rm low} = 0.4632 \pm 0.0041$ Å^2 for reflections up to 880 [$(\sin\theta)/\lambda = 1.04$ Å^{-1}], in excellent agreement with previous measurements, and $B_{\rm high} = 0.5085 \pm 0.0035$ Å^2 for reflections higher than 10 10 0 [$(\sin\theta)/\lambda \geq 1.30$ Å^{-1}]. We also find no anharmonic contribution to the temperature factor of F_h within the limit of accuracy of the experiment, in good agreement with previous x-ray measurements and some neutron measurements, but in contradiction to some of the neutron forbidden-222-reflection results.

I. INTRODUCTION

The charge distribution in a perfect single silicon crystal has recently received much experimental[1–9] and theoretical[10–15] attention, which has been further stimulated by the renewed interest in the thermal behavior of atoms,[16,17] the band structure of semiconductors, and the scattering process of radiation by crystalline material. The systematic sets of measured structure factors by De Marco and Weiss[2], Hattori *et al.*,[1] and, in particular, the high-precision ones of Tanemura and Kato, Kato and Tanemura,[3] and Aldred and Hart[4] proved to be invaluable in elucidating the details of the charge distribution in silicon. The most extensive of these, that of Aldred and Hart[4] (AH), has been repeatedly[4,13,14] used to test the validity of various theoretical models proposed for the charge distribution of silicon atoms in the crystals. The 10^{-3}-electron level of accuracy achieved proved to be sufficiently high for the determination of the nonspherical centrosymmetric and antisymmetric corrections to the free-atom spherical charge distribution, the effective harmonic vibrational amplitude of the atom, the upper limit to the anharmonic component of the effective one-atom potential, and the superiority of the Kohn-Sham-Gaspar exchange term[18] over the Slater[19] one in the orthogonalized-plane-wave (OPW) band-structure calculations of Stuckel and Euwema,[12] and also led to the detection of an unsuspected expansion of the valence shell by a few percent.[4,13] All high-precision structure factor measurements mentioned above were done by variants of the Pendellosung[20] method using film detection, which, although capable of achieving a few thousandths of an electron per atom accuracy in F_h determination, is difficult, through lack of intensity, to apply to high-order reflections. For this reason, no high-accuracy structure factors have been published for reflections higher than 880, i.e., for $(\sin\theta)/\lambda > 1.0416$ Å^{-1}. Thus, a number of important issues, especially the relativistic effects on the inner-core wave functions, the magnitude of the anharmonic term in the effective one-particle potential of the atom, and the temperature and momentum transfer behavior of the Debye-Waller factor (the contributions of which are particularly large at high-order reflections), remained outside the reach of high-accuracy x-ray measurements.

A few years ago Bonse and co-workers[8,21] proposed a variant of the Pendellosung method for obtaining the structure factor F_h from the fine structure of Laue-case rocking curves of two thin crystals. This technique employs photon counting, which is faster and more reliable than film detection. Their separated-crystal measurements achieved accuracies of only $\sim 15 \times 10^{-3}$ e/atom due to the uncertainties in the crystal thickness measurements, even for the low-order 440 reflection. They were also confronted with stability problems which are particularly serious for the subsecond-of-arc fringe widths obtained even in medium-order reflections from silicon. Least-squares fitting of data to theory is quite impossible in the presence of drift.

In a very recent paper, published while the present paper was in its final draft, Teworte and Bonse[22] (TB) report structure factors for 16 reflections ranging from 111 to 880 for Ag $K\alpha_1$ and Mo $K\alpha_1$ radiations, measured using a separated-crystal Laue-Laue diffractometer. All of these reflections, except two, were previously measured by

Aldred and Hart,[4] and the two sets agree to within the experimental errors for all points. Note that the errors quoted by Teworte and Bonse for their own data are probable errors, i.e., 0.6745σ, where σ is the standard deviation, while those they quote for the Aldred and Hart data are root-mean-square deviations. Assuming for the moment that the root-mean-square deviations are equal to the standard deviations, and calculating the mean σ given by

$$\bar{\sigma}=\frac{1}{N}\sum_{i=1}^{N}(\sigma_i/F_i)\ ,$$

where the summation goes over all N reflections, and F_i and σ_i are the structure factor and its standard deviation for the ith reflection, respectively, we obtain, for the Teworte and Bonse data, $\bar{\sigma}^{\mathrm{TB}}_{\mathrm{Ag}\,K\alpha}=0.001\,35$ and $\bar{\sigma}^{\mathrm{TB}}_{\mathrm{Mo}\,K\alpha}=0.001\,34$, while for the Aldred and Hart room-temperature data we obtain $\bar{\sigma}^{\mathrm{AH}}_{\mathrm{Ag}\,K\alpha}=0.001\,46$ and $\bar{\sigma}^{\mathrm{AH}}_{\mathrm{Mo}\,K\alpha}=0.001\,37$. The difference in accuracy between the two experiments appears to be marginal at best. However, in their detailed analysis, Price *et al.*[14] pointed out that the errors quoted by Aldred and Hart for their own data are root-mean-square deviations of the 20 individually measured values *from* the mean, rather than the standard deviations *in* the mean, σ.

The actual values of σ for the Aldred and Hart data are therefore smaller by a factor of $(20-1)^{1/2}\approx 4$ than those quoted in Refs. 4 and 22, which would make them smaller than those of Teworte and Bonse[22] by a factor of 3—4. The incompatibility of the claimed accuracy of the Teworte and Bonse data versus the Aldred and Hart data is graphically demonstrated by Fig. 6 in Ref. 22, where although the TB data carry smaller error bars than those of the BH data, due to the difference between the rms deviations and the probable errors, as discussed above, the scatter in the data points about the straight line fitted to them is actually *larger* for the TB data than for the BH data. This is borne out by the relative errors in the slope and the intercept of the fitted line, calculated by Teworte and Bonse for their own, and for the data of AH. These are 60% and 11% for the TB data and 23% and 7.5% for the AH data. The above discussion indicates that the factor-of-2 improvement in accuracy claimed by Teworte and Bonse[22] over the ten year old data of Aldred and Hart[4] is unsubstantiated by the errors they quote for their data.

Recently, a novel monolithic thin-crystal diffractometer was developed by Cusatis *et al.*[7] and the present authors,[9] which, in conjunction with energy-dispersive data collection and nonlinear least-squares computer fitting techniques, proved capable of achieving thousandths-of-an-electron accuracies in atomic scattering factor determination even for high-order reflections. The method was fully discussed in a previous publication[9] along with some preliminary data.

Here we present the full results of a study of high-order scattering factors. A set of eight structure factors ranging from 444 [$(\sin\theta)/\lambda=0.637\,83$ Å^{-1}] up to 14 14 0 [$(\sin\theta)/\lambda=1.8228$ Å^{-1}] were measured, and those up to 12 12 0 are interpreted for a number of wavelengths to an accuracy of a few thousandths of an electron. The general method and the monolithic double-crystal diffractometer used in these measurements are briefly described in the next section; Sec. III contains a summary of the necessary basic structure-factor formalism of Dawson.[10] In Sec. IV the structure factors obtained are presented along with some relevant theoretical results, followed by a full discussion in Sec. V.

II. EXPERIMENTAL METHOD

The Laue-case rocking curves of two thin, perfect crystals are known to exhibit fine structure.[7,8,21–23] The details of this structure are extremely sensitive to the value of the structure factor F_h for the plane and wavelength used. Thus it is possible, under practical conditions, to determine the structure factor experimentally from the measured rocking curve to an accuracy of about 1×10^{-3} e/atom. This is the basic idea behind the method used in the measurements reported here.

For symmetric Laue-case geometry, the intrinsic reflection curve is given by[24]

$$I_R(y)=\exp(-\mu t/\cos\theta_B)\,|\sin[(\pi t/\Delta_0)(y^2+\nu^2)^{1/2}]/(y^2+\nu^2)^{1/2}|^2\ , \tag{1a}$$

where

$$\nu^2=\chi_h\chi_{\bar{h}}/|\chi_h\chi_{\bar{h}}|\ .$$

χ_h is the complex electric susceptibility. For silicon, where $\mathrm{Re}\chi_h>\mathrm{Im}\chi_h$, Eq. (1a) can be written as[25]

$$I_R(y)=[\exp(-\mu t/\cos\theta_B)/2(1+y^2)]\{\cosh[\mu t\epsilon(1+y^2)^{-1/2}/\cos\theta_B]-\cos[(2\pi t/\Delta_0)(1+y^2)^{1/2}]\}\ , \tag{1b}$$

where μ, t, and θ_B are the linear coefficient of absorption, the crystal thickness, and the Bragg angle, respectively. y is the angular parameter, and Δ_0 is the extinction length given by[25]

$$y=(\theta-\theta_B)(\sin2\theta_B)/(C\,|\chi_{hr}|),\quad \Delta_0=\lambda(\cos\theta_B)/(C\,|\chi_{hr}|)\ .$$

Here, θ is the glancing angle for a given ray, λ is the wavelength, and C is the polarization factor,

$$C=\begin{cases}1, & \sigma \text{ polarization}\\ |\cos 2\theta_B|, & \pi \text{ polarization.}\end{cases}$$

χ_h for silicon is given by

$$\chi_h=\chi_{hr}+i\chi_{hi}=(r_e\lambda^2/\pi V)|F_h|+i(\mu\lambda/2\pi)\epsilon\ ,$$

where r_e is the classical electron radius, V is the unit-cell volume, F_h is the temperature modified structure factor, and ϵ is the temperature modified ratio $|\chi_{hi}|/|\chi_{0i}|$:

$$\epsilon=\epsilon_0\exp(-M)=\begin{cases}a_g\exp(-M)(1-2q\sin^2\theta_B), & \sigma \text{ polarization}\\ a_g\exp(-M)[(1-q)\cos 2\theta_B+q\cos 4\theta_B], & \pi \text{ polarization.}\end{cases} \quad (2)$$

$M=B(\sin\theta_B/\lambda)^2$ is the Debye-Waller factor and $a_g=1$ if all Miller indices of the plane used are even and $h+k+l=4n$; $a_g=1/\sqrt{2}$ if all indices are odd and $a_g=0$ for any other combination.[22] q is a constant related to the photoelectric absorption coefficient. For thickness t of order of a few Δ_0 and μt of order unity, the reflection curve given in Eq. (1b) will exhibit oscillatory structure due to the cosine term. For the range of wavelengths and planes investigated here, the difference between Eq. (1a) and the approximate Eq. (1b) was found, by computer simulations, to be negligible. Note that the Debye-Waller factor is included in two different quantities: ϵ and F_h. The significance of this will be discussed later.

If we assume the radiation source to be unpolarized, the measured rocking curve is given by the sum of the convolutions of two intrinsic reflection curves of the two polarization states:

$$I(\Delta)=I_0\sum_{\sigma,\pi}\int I_R^{\sigma,\pi}(\theta)I_R^{\sigma,\pi}(\theta+\Delta)d\theta\ , \quad (3)$$

where Δ is the angle of rotation of one crystal relative to the other.

The structure factor F_h for a given plane and wavelength is obtained from the measured rocking curve by fitting Eq. (3) to the data using a multiparameter nonlinear least-squares procedure[26] which optimizes both F_h and the thicknesses t_1 and t_2 of both crystals. Convergence is well below 0.1% for all parameters optimized. This procedure eliminates the need for a separate measurement of t_1 and t_2, which is the dominant source of error in the previous as well as the very recent F_h measurements of Bonse and Teworte.[8,22] The value of q used in the fitting was linearly interpolated from those of Hildebrandt *et al.*[27] The μ values were interpolated using the Victoreen relation[28] from the measured values of Hildebrandt *et al.*[29] The Debye parameter $B=0.4680$ Å^2 obtained by Price *et al.*[14] from a full matrix least-squares refinement of the Aldred and Hart[4] data were employed for calculating ϵ in Eq. (1).

The monolithic double-crystal diffractometer used to measure the rocking curves is shown in Fig. 1. Its "two crystals" are nominally 275-μm-thick wafers carved out of a single block of perfect silicon crystal. A rotation of one wafer relative to the other is done by bending a leaf spring cut into the monolith in between the wafers using a linear[29] force transducer made of an electromagnet and a small permanent rare-earth, epoxy-bonded magnet attached to the blocks carrying the wafers. Such an arrangement allows extremely high resolution, and repeatable and smooth[30] rotations to be carried out electrically rather than mechanically with a corresponding high immunity to vibrations, temperature variations, etc. Stability was better than 0.001 seconds of arc per day.

The use of an energy-dispersive Ge detector in conjunction with the continuous radiation from a tungsten target x-ray tube made possible the simultaneous measurements of a series of rocking curves of the same family by recording the various harmonics separately. This procedure not only decreases measurement time considerably, but also minimizes the influence of possible sources of errors such as residual drifts, small nonlinearities in the scan, etc., which influence all harmonics equally, thus leaving the ratios of the deduced structure factors unchanged. More conventional single-wavelength scans with Mo $K\bar{\alpha}$ and Ag $K\bar{\alpha}$ radiations were also done. Unlike separated-crystal diffractometers,[8,22] the monolith is highly immune to vibrations, and simple rubber pads inserted between the θ_B-defining rotary table and the table carrying the x-ray tube were found to render any vibrationally induced smearing of the oscillatory patterns undetectable. The monolith was shielded from room-temperature vibrations by a polystyrene enclosure and two metallic ones. The temperature was monitored by the microcomputer controlling the experiment,[31] and varied by less than 0.1 K during a 12-h data run. Data collection was done in the signal-averaging mode[32] to minimize the influence of possible source-intensity drifts.

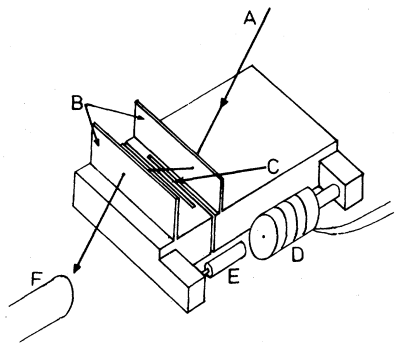

FIG. 1. Monolithic thin-wafer Laue case diffractometer; *A*, x-ray beam; *B*, wafers; *C*, leaf spring; *D*, electromagnet; *E*, permanent magnet; *F*, solid-state detector.

TABLE I. Measured structure factors per atom, F_h/Q, for silicon, and the corresponding theoretical values calculated using relativistic-Hartree-Fock wave functions (f_{RHF}) and the dispersion corrections of Cromer and Liberman (Ref. 43) (f'_{CL}) and Cusatis and Hart (Ref. 41) (f'_{CH}). For details, see text.

$h\,k\,l$		$(\sin\theta)/\lambda$ (Å^{-1})	E (keV)	λ (Å)	f_{RHF}	f'_{CL}	f'_{CH}	$(F_h/Q)_{\mathrm{CL}}$	$(F_h/Q)_{\mathrm{CH}}$	$(F_h/Q)_{\mathrm{meas}}$
444	*a*	0.637 83	13.956	0.8884	4.9835	0.1072	0.1209	4.2113	4.2226	4.2437±0.0093
	b		17.687	0.7010		0.0693	0.0840	4.1799	4.1921	4.2062±0.0085
660		0.781 18	16.587	0.7477	3.8854	0.0786	0.0932	2.9820	2.9930	3.0030±0.0097
880	*a*	1.041 57	23.262	0.5330	2.5539	0.0372	0.0511	1.5618	1.5701	1.5719±0.0021
	b		29.492	0.4204		0.0175	0.0290	1.5499	1.5568	1.5613±0.0043
777	*a*	1.116 21	17.445	0.7107	2.3022	0.0715	0.0863	1.3270	1.3353	1.3283±0.0042
	b		22.109	0.5608		0.0425	0.0568	1.3108	1.3188	1.3080±0.0023
	c		24.426	0.5076		0.0326	0.0461	1.3053	1.3129	1.3053±0.0034
888	*a*	1.275 66	17.445	0.7107	1.9216	0.0715	0.0863	0.9324	0.9393	0.9038±0.0030
	b		22.109	0.5608		0.0425	0.0568	0.9188	0.9255	0.8915±0.0020
	c		27.912	0.4442		0.0215	0.0337	0.9090	0.9147	0.9019±0.0044
10 10 0	*a*	1.301 97	17.445	0.7107	1.8689	0.0715	0.0863	0.8794	0.8861	0.8294±0.0010
	b		22.109	0.5608		0.0425	0.0568	0.8663	0.8728	0.8744±0.0026
	c		25.303	0.4900		0.0298	0.0430	0.8606	0.8665	0.8921±0.0120
	d		27.638	0.4486		0.0222	0.0345	0.8571	0.8627	0.9217±0.0062
	e		29.077	0.4264		0.0185	0.0302	0.8555	0.8608	0.9379±0.0080
999		1.435 12	22.109	0.5608	1.6752	0.0425	0.0568	0.6566	0.6620	0.6126±0.0032
12 12 0		1.562 36	22.109	0.5608	1.5400	0.0425	0.0568	0.5061	0.5107	0.4577±0.0011

A sum of seven 12-h runs collected in the energy-dispersive mode for a series of $h\,h\,0$ planes at $\theta_B=30°$ is plotted in Fig. 2. The high stability and repeatability of the monolith is manifested in the sharp, unsmeared features, the high contrast, and the fact that the curves are completely symmetric within the statistical accuracy limits of the data. This last feature is convincing proof of the absence of angular drifts which plague separated-crystal spectrometers, as indicated by the asymmetric rocking curves of Ref. 8. Moreover, it is an indispensible tool in identifying spurious structure resulting from simultaneous reflections or any other source. Note the structure seen in the 10 10 0 curve at $\Delta=0.122$ seconds of arc to the right of the central peak. Its absence from the same position to the left of the peak identifies it as being spurious. Note also the fast decrease in the widths of the curves as the order of the plane increases. The finite dynamic range of the linear force transducer limits the number of curves which can be measured *simultaneously* with reasonable resolution. It is, however, sufficiently easy to alter the magnet current range so as to cover a very wide range of planes with adequate resolution by a small number of sets of such simultaneous measurements, with ample overlap between sets to ensure complete consistency. Another effect seen in the figure is the decrease in the amount of structure with the increase of the order of reflection. This is due to the increase in the extinction length as both the wavelength of the harmonics used for the higher-order planes and their F_h values decreases. Since the fitting procedure locks into the shape rather than the absolute intensity of the curve, the absence of structure gradually impairs convergence and eventually limits the order of the rocking curve which can be analyzed for a given t_1, t_2, and λ. In such cases the obvious solution is to increase the crystal thickness, i.e., the ratio t/Δ_0. On the other hand, an increase in t causes a corresponding decrease in the intensity due to absorption, thus lowering the amount of structure in the outer wings of the rocking curve which can be detected above a given level of statistical noise. Owing to the complicated relations between the various parameters involved, it is difficult to set precise analytic limits on t.

The data in Table I indicate, however, that even for extinction lengths as large as $\Delta_0=550$ μm, wafers with $t=275$ μm, i.e., $t/\Delta_0\approx0.5$, corresponding to the 999 reflection with Ag $K\bar{\alpha}$ radiation, are sufficiently thick to allow high-accuracy determination of F_h. Even for the 14 14 0 curves, with $\lambda=0.3205$ Å, for which the extinction length was $\Delta_0=2$ mm, one fringe was found on each side of the central peak. Note that in this case, $t/\Delta_0=0.14$. Absorption also imposes some limits on t. While our measurements extended only up to $\mu t=3$ (440 at $\theta_B=48°$), where well-defined fringes were obtained, in the closely related traverse Pendellosung measurements of Fehlmann and Fujimoto,[1] fringes were obtained for $\mu t\geq4.5$.

In view of the above discussion, the limits of[22] $\mu t\leq1$–2 and t larger than several times[8] Δ_0, given by Teworte and Bonse for their separated-crystal measurements, seem to be too restrictive. Those limits were, however, dictated by the quality of their data and by the method of analysis employed, in which F_h is extracted from the height of the extrema on the outer parts of the wings of the rocking curves, so as to minimize the influence of angular drifts[8] on their final results. They require, therefore, a large number of fringes in an angular range where the intensity is much smaller than in the vicinity of $\Delta=0$. Thus, it is crucial to limit both absorption and the ratio t/Δ_0 severely. In contrast, the stability of our monolithic diffractometer, and its high immunity to external influences, which is manifested in completely symmetric and high-contrast rocking curves, allows computer fits to the complete curve to be carried out. Thus, we are able to obtain high-accuracy structure factors even where only few fringes are present in the rocking curves, as demonstrated in Figs. 4–6. Further details and a full discussion of our method are given in Ref. 9.

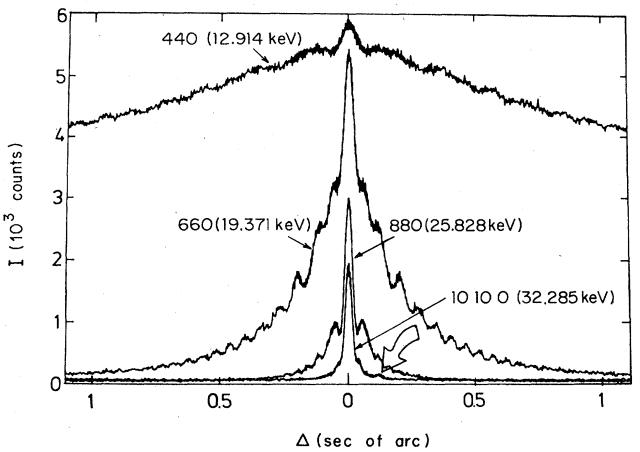

FIG. 2. Family of $h\,h\,0$ rocking curves measured simultaneously in the energy-dispersive mode with $\theta_B=30°$. The plot is the sum of seven 12-h data runs. Note the sharp features, and the complete symmetry which indicates high stability. A spurious structure is seen in the 10 10 0 curve at $\Delta=0.122$ seconds of arc to the right of the central peak (indicated by an arrow).

III. STRUCTURE FACTOR

For an atom in a crystal having a charge density $\rho(\vec{r})$, the atomic scattering amplitude is defined by[10]

$$f(\vec{k})=\int_{\text{atom}}\rho(\vec{r})\exp(i\vec{k}\cdot\vec{r})dv\ .$$

Following Dawson,[10] we assume that the charge distribution follows the site symmetry of the atoms, which is $\bar{4}3m$ (T_d) in silicon. This leads to a nonspherical charge distribution, which can be written as

$$\rho(\vec{r})=\bar{\rho}_c(\vec{r})+\delta\rho_c(\vec{r})+\rho_a(\vec{r})\ ,$$

where the first term is spherically symmetric, the second is centrosymmetric but not spherically symmetric, and the third is antisymmetric. The atomic scattering amplitude will have a corresponding form,

$$f(\vec{k})=\bar{f}_c(k)+\delta f_c(\vec{k})+f_a(\vec{k})\ .$$

Note that the spherically symmetric term $\bar{f}_c(k)$ includes the usual dispersion correction term $f'(\lambda)$, and

TABLE II. Theoretical silicon structure factor data in Dawson's formalism (Ref. 10).

$h\,k\,l$	$(\sin\theta)/\lambda$ (Å^{-1})	Q	a	b	c	d	A_3	$10^4\langle j_3\rangle$	B_4	$10^4\langle j_4\rangle$	$10^2 B_6$	$10^4\langle j_6\rangle$
4 4 4	0.63783	−8	+1	0	0	−1	0.1924	−208.2	−0.2667	626.5	1.538	1970
6 6 0	0.78118	−8	+1	0	0	−1	0	−71.82	−0.1	227.4	−1.407	817.6
8 8 0	1.04157	+8	+1	0	0	−1	0	−16.40	−0.1	53.95	−1.407	215.4
7 7 7	1.11621	$-4\sqrt{2}$	+1	+1	+1	−1	0.1924	−11.54	−0.2667	38.17	1.538	154.9
8 8 8	1.27566	+8	+1	0	0	−1	0.1924	−5.863	−0.2667	19.58	1.538	81.47
10 10 0	1.30197	−8	+1	0	0	−1	0	−5.288	−0.1	17.68	−1.407	73.80
9 9 9	1.43512	$-4\sqrt{2}$	+1	−1	−1	−1	0.1924	−3.233	−0.2667	10.87	1.538	45.98
12 12 0	1.56236	+8	+1	0	0	−1	0	−2.101	−0.1	7.105	−1.407	30.37

$k=4\pi(\sin\theta)/\lambda$ is the momentum transfer. The two correction terms to the spherical charge distribution can be expanded in Kubic harmonics,[33] yielding

$$f_a(\vec{k})=f_{a,3}(\vec{k})+f_{a,7}(\vec{k})+\cdots ,$$

$$\delta f_c(\vec{k})=\delta f_{c,4}(\vec{k})+\delta f_{c,6}(\vec{k})+\cdots ,$$

where

$$f_{a,i}(\vec{k})=-A_i a_i\langle j_i\rangle ,\quad \delta f_{c,i}(\vec{k})=B_i b_i\langle j_i\rangle , \tag{4}$$

a_i and b_i are constant, and

$$A_3=hkl/(h^3+k^2+l^2)^{3/2} ,$$
$$B_4=(h^4+k^4+l^4)/(h^2+k^2+l^2)^2-\tfrac{3}{5} , \tag{5}$$
$$B_6=A_3^2+B_4/22-\tfrac{1}{105} ,$$

where h, k, and l are the Miller indices of the plane involved. $\langle j_i\rangle$ is

$$\langle j_i(k)\rangle=(-1)^i 4\pi\int_0^\infty r^{p+2}\exp(-\alpha r^m) j_i(kr)\,dr , \tag{6}$$

where j_i is the spherical Bessel function of order i. For silicon, Dawson obtained,[10] using pre-1970 data,

$$p=2,\quad m=2,\quad \alpha=0.88\ \text{Å}^{-2},\quad a_3=1.11,\quad b_4=-0.32 . \tag{7}$$

The structure factor $F_h\equiv F(hkl)$ is written in the Dawson formalism as

$$F_h=Q(af_cT_c+bf_aT_c+cf_cT_a+df_aT_a) , \tag{8}$$

where, in the above notation,

$$f_c=\bar{f}_c+\delta f_{c,4}+\delta f_{c,6}+\cdots ,$$

$$f_a=f_{a,3}+f_{a,7}+\cdots ,$$

$Q=8a_g$, and a, b, c, and d are ±1 or 0 depending on h, k, and l. T_a and T_c are temperature factors whose explicit form depends on the effective one-particle potential assumed. Since, here, the main anharmonic term is third order, the simplest potential is of the form

$$V(r)=V_0(r)+\tfrac{1}{2}\alpha(x^2+y^2+z^2)+\beta xyz .$$

As shown by Dawson and Willis,[34] this yields the temperature factors

$$\begin{aligned} T_c&=\exp(-k^2k_BT/2\alpha)=\exp\{-B[(\sin\theta)/\lambda]^2\}\\ &=\exp(-M) ,\\ T_a&=T_c(k_BT)^2(8\pi^3/V)(\beta/\alpha^3)hkl , \end{aligned} \tag{9}$$

where k_B is the Boltzmann constant. The second Miller index and the momentum transfer, both denoted k for reasons of convention, should not be confused. At room temperature,[4,35] $\alpha=7.85\times10^{-12}$ ergs Å^{-2}. β can be determined, in principle, by temperature-dependent neutron measurements of the "forbidden" 222 reflection. The situation at present is, however, rather unclear. Nunes[36] derived an upper limit of $\beta<0.5\times10^{-11}$ ergs Å^{-3} from such measurements. Aldred and Hart[4] reduced this limit by a factor of 2, using their high-accuracy structure factor

data. In contrast, the neutron 222 integrated reflectivity data of Roberto *et al.*[5] yield a definite value of $\beta=(0.542\pm0.054)\times10^{-11}$ ergs Å^{-3}. For this value of β,

$$T_a/T_c=2.7\times10^{-5}hkl \tag{10}$$

at room temperature. For the highest-order $h\,h\,h$ reflection measured by us, 999, this is a 2% effect, well above the experimental error; it should, therefore, be clearly detectable.

Since[37]

$$j_n(z)=[\pi/(2z)]^{1/2}J_{n+1/2}(z)\ ,$$

where J is the Bessel function, for $m=2$, Eq. (6) can be written as

$$\langle j_i(k)\rangle=(-k/2)^i\pi^{3/2}\alpha^{-\nu}[\Gamma(\nu)/\Gamma(\eta)]\times M(\nu,\eta,-k^2/4\alpha)\ ,$$

where Γ denotes the usual Γ function, $\nu=(p+i+3)/2$, $\eta=i+\frac{3}{2}$, and M is the confluent hypergeometric function for which tables[38] and computer routines[39] are available. The values of $\langle j_i\rangle$, $i=3,4,6$, and the other quantities discussed in this section are listed in Table II for the planes investigated here.

IV. RESULTS

The sum of twelve 1-h scans of a set of $h\,h\,0$ planes done in the energy-dispersive mode with 880 reflecting the Ag $K\bar{\alpha}$ wavelength is given in Fig. 3. For the data presented in this figure, the known[4] structure factor of 880 was employed in fitting the 880 data to the theoretical curve. This fit yields the effective thickness t_1 and t_2 traversed by the beam. Since all rays, regardless of wavelength, follow the same physical path, these values of t_1 and t_2 apply to all the other $h\,h\,0$ reflections as well, and were employed in the fit of the 440, 660, 10 10 0, and 12 12 0 data, this time optimizing F_h. This procedure was repeated for five 1-h scans, and the value adopted for F_h was the mean of the individual values, each adjusted to a temperature of 293.2 K using the actual mean temperature recorded for each scan. The standard deviation σ in this value was calculated from the scatter of the five values, taking into account the σ of each individual F_h as obtained from the fitting program. The same procedure was used in the analysis of all other data sets measured. The (440), (660), or (880) plane, the F_h for all of which is known to high accuracy, was set to reflect the characteristic wavelength, and the corresponding curve was used to obtain t_1 and t_2. These, in turn, were used to calculate F_h for the other simultaneously measured planes. For further details, see Ref. 9. In the data plotted in Fig. 3 the transducer's dynamic-range limitations rendered the measurable portion of the 440 curve insufficient to support a meaningful fit. The same holds for the 12 12 0 and 14 14 0 curves, which lack structure. For the 10 10 0 curve in this set, however, and for other planes in the numerous data sets measured, the agreement between the optimized theoretical curves and the measured ones is very good. An example of one data set out of the 12 included in Fig. 3 is given in Fig. 4(a) for the 10 10 0 curve. As shown in Fig. 4(b), all residuals are well within the statistical 2-standard-deviation (2σ) levels of the measured data and are randomly distributed. The F_h values of Table I are the mean of several fits like the one presented in Fig. 4.

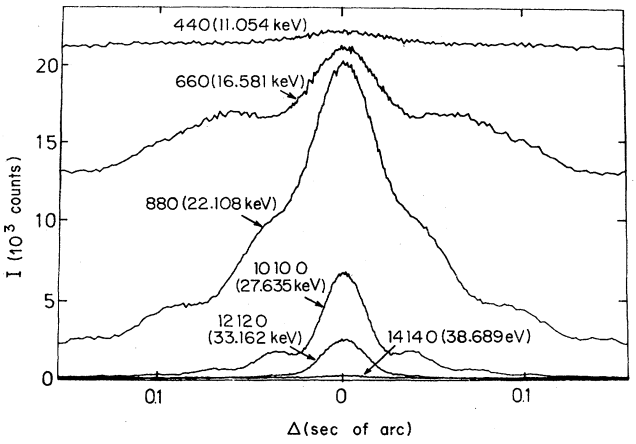

FIG. 3. Family of $h\,h\,0$ rocking curves measured with high resolution in the energy-dispersive mode. The plot is a sum of twelve 1-h data sets. Note the large decrease in the widths and the gradual fading out of structure with increasing order of reflection. The 440 and 660 curves were shifted upwards in the plot by 15 000 and 5500 counts, respectively. Peak intensities for the 440 and 660 curves are smaller than for 880 because of the shape of the continuous spectrum of the source, as well as the increased absorption at longer wavelengths.

Two other examples are given in Figs. 5 and 6. The 12 12 0 rocking curve in Fig. 5 was measured with characteristic Ag $K\bar{\alpha}$ radiation. Note that most of the structure in this very-high-order reflection has already faded out because of the large extinction length. What is left, however, is sufficient to ensure good convergence, as evidenced by the low level of residuals in Fig. 5(b). The same high-quality fit is obtained in much more oscillatory curves, an example of which is given in Fig. 4 of Ref. 9. The 888 curve in Fig. 6 was measured in the energy-dispersive mode with the (555) planes reflecting the Mo $K\bar{\alpha}$ wavelength. Note the structure at 0.14 seconds of arc to the left of the central peak (marked by an arrow in the figures). Its absence from the same position to the right of the peak proves it to be spurious. The residuals at this position are therefore quite large. Nevertheless, the quality of the fit in other peaks of the curve, and, consequently, the value of F_h deduced, are not affected, as is borne out by the randomly distributed and 2σ-limited residuals in Fig. 6(b) at all points except in the immediate vicinity of the spurious structure. This immunity to localized spurious structure is an important advantage of methods which fit the complete measured rocking curve over partial fitting of only the relative heights of the maxima and minima on the outer flanks of the curve, as done in the separated-crystal measurements of Bonse and Teworte.[8,22] To some extent, this "distribution of systematic error" renders a separate physical elimination of coherent simultaneous Bragg reflections unnecessary. As the captions to Figs. 4–6 indicate, the computer fit allows crystal thickness determinations to well below 0.1 μm, which has not

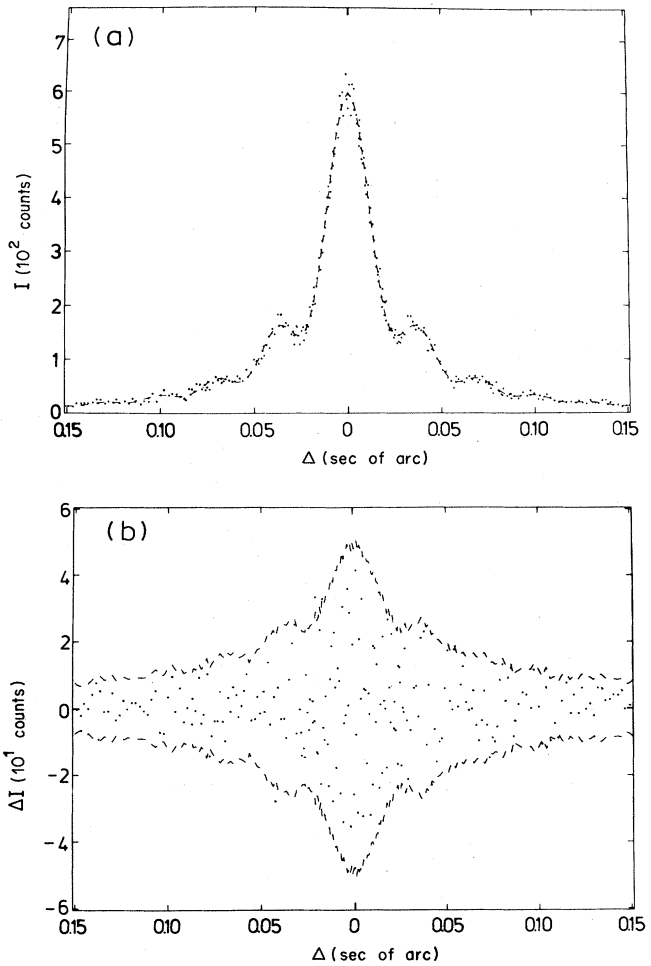

FIG. 4. 10 10 0 rocking curve; *one* of the twelve data sets included in Fig. 3. (a) Experimental (dots) and fitted theoretical (dashed line) rocking curves for $F_{10\,10\,0}=0.9216$, $t_1=(282.53\pm0.11)$ μm, and $t_2=(274.79\pm0.09)$ μm. (b) Fit residuals. The difference between theory and experimental (dots) are randomly distributed and within the statistical $\pm2\sigma$ levels of the data (dashed line). Note that the F_h values of Table I are the mean of those obtained from several fits like the one presented in this figure.

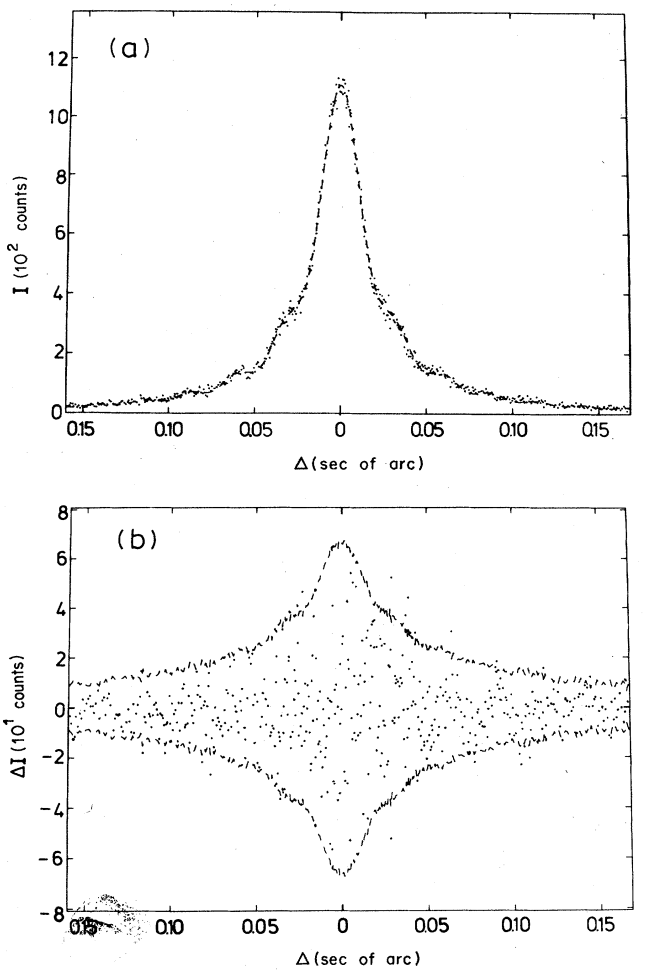

FIG. 5. Single 12 12 0 rocking curve measured with characteristic Ag $K\bar{\alpha}$ radiation. For notation, see Fig. 4. The fit parameters are $F_{12\,12\,0}=0.4570$, $t_1=(232.58\pm0.082)$ μm, and $t_2=(293.22\pm0.10)$ μm. Note the relative lack of structure when compared to Figs. 4 and 6 due to the large extinction length. Note also the <0.1-μm accuracy in thickness, obtained from the fit, which has not yet been achieved by direct measurement.

been achieved in contact methods.

The complete set of structure factors measured in this study is given in Table I. The fact that our new scattering amplitude values for the 880 curve agrees with those of Aldred and Hart[4] is not an inevitable result of our algorithm, but rather a clear confirmation of the repeatability of experiments and of proper convergence of the least-squares program. Theoretical spherical atom scattering amplitudes, denoted f_{RHF}, were interpolated from the relativistic-Hartree-Fock (RHF) values listed in the *International Tables for X-ray Crystallography.*[40] Since at least four different studies[4,14,41,42] indicate that the dispersion corrections of Cromer and Libermann[43] (f'_{CL}) do not agree with experiment at short wavelengths, we have listed in Table I those of Cusatis and Hart[41] (f'_{CH}) as well. Unfortunately, these absolute, measured dispersion corrections were published[41,42] only for Mo $K\alpha_1$ and Ag $K\alpha_1$ wavelengths. Although relative $f'_\lambda - f'_{\mathrm{Ag}\,K\alpha_1}$ Pendellosung measurements[44] are also available for several characteristic wavelengths λ, none of these coincide with those listed in Table I. The values of f'_{CH} for wavelengths other than Mo $K\alpha$ and Ag $K\alpha$ were, therefore, linearly extrapolated from those two values. The structure factors were calculated using both CL and CH values for the dispersion correction for each wavelength. These, denoted $(F_h/Q)_{\mathrm{CH}}$ and $(F_h/Q)_{\mathrm{CL}}$, include a nuclear scattering amplitude[3] of 3.8×10^{-3} e/atom and the Debye parameter[14] $B=0.4680$ Å^2. As for the correction terms to the free-atom-scattering amplitude, the experimental[4] values of $a_3=1.012$ and $b_4=0.206$, and the transforms listed in Table II, yield, for all planes except 444, $f_{a,3}$ and $\delta f_{c,4}$ below the experimental accuracy of our experiment. These correction terms are of no consequence for the 444 curve, since although here $\delta f_{c,4}=2.8\times10^{-3}$ e/atom, the

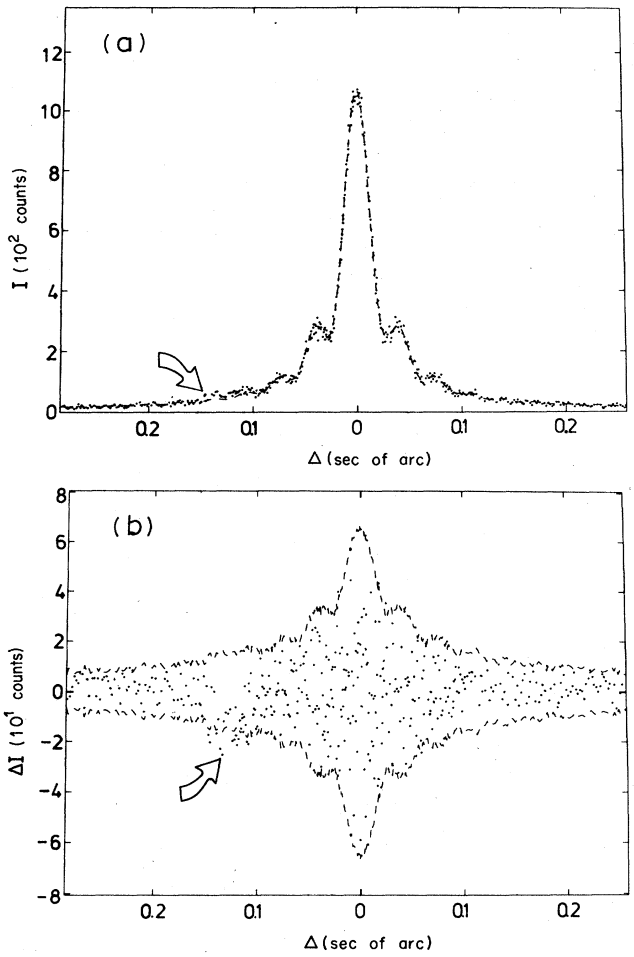

FIG. 6. 888 rocking curve measured in the energy-dispersive mode with $\theta_B = 34.52°$. For notation, see Fig. 4. The fit parameters are $F_{888} = 0.9002$, $t_1 = (268.49 \pm 0.071)$ μm, and $t_2 = (278.67 \pm 0.055)$ μm. The spurious structure discussed in the text at $\Delta = 0.14$ seconds of arc to the left of the peak is indicated by an arrow in both (a) and (b). Note that the quality of the fit in other parts of the curve is not impaired.

term bf_aT_c is equal to 0.

Finally, the last column of Table I lists the measured values of F_h/Q. The unusually large experimental errors in F_{444} and F_{660} reflect the restricted dynamical range of the force transducer, as discussed earlier. The fading out of structure at short wavelengths and in high-order reflections is responsible for the slightly larger σ of F_{10100} (at $\lambda = 0.4486$ and at 0.4268 Å). The $\lambda = 0.4900$ Å data set for the 10100 reflection was measured without the thermal enclosure, which accounts for the increased standard deviation in that case.

V. DISCUSSION

The most intriguing feature of the measured F_h data is the large deviation from the theoretical values for high $(\sin\theta)/\lambda$. In view of the excellent agreement with both theory and previous high-precision F_h measurements,[4] which we obtain for the low-$(\sin\theta)/\lambda$ (444), (660), and (880) planes for all wavelengths measured, we believe that it is highly improbable that the deviations are caused by a systematic error in the experiments or in the data analysis.

Strains in the crystal cannot account for these deviations either. Although, to our knowledge, no detailed theoretical or experimental studies of the influence of strain on thin-crystal Laue-case rocking curves have been published, Bonse and Teworte[8,22] briefly consider the subject and conclude that even very low inhomogeneous strain levels or homogeneous strains which are unequal in the two crystals are bound to smear out the structure in the curves and render them asymmetric. Since the observed contrast was very close to the theoretical one in all our rocking curves, and since no asymmetry was detected, such strain gradients can clearly be ruled out. This was also verified by a number of double-crystal Laue topographs taken with Ag $K\bar{\alpha}$ and 660 and 880 Bragg reflections in the $h\,h\,0$ diffractometers and using the 555 Bragg reflection in the $h\,h\,h$ diffractometers. Moreover, in the closely related Pendellosung measurements, strains were found[4] to cause a smaller fringe spacing, which, in turn, results in a *higher* value being deduced for F_h than in the unstrained crystal. This last effect was indeed detected in our experiments in a number of 10100 data sets measured using a series of decreasing wavelengths. These are the 10100 (labeled a—e) values listed in Table I and plotted in Fig. 7. Near the point where the x-ray beam is incident

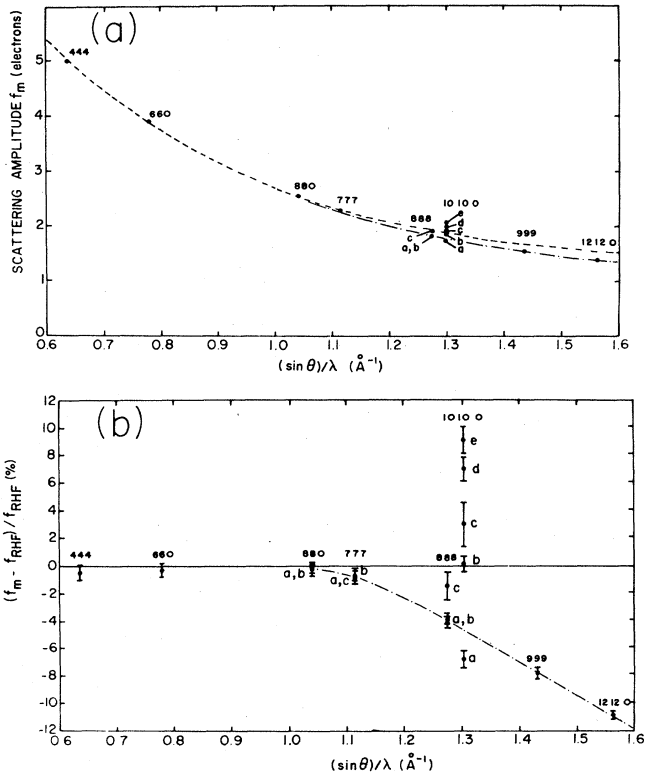

FIG. 7. Atomic-scattering amplitude f_m calculated from $(F_h/Q)_{meas}$ and f'_{CH} of Table I assuming $B = 0.4680$ Å^2. (a) f_m, dots; f_{RHF}, dashed line. (b) The relative difference between theory and experiment. Note the smoothly increasing deviation from zero for $(\sin\theta)/\lambda > 1.1$ Å^{-1} (dashed-dotted eye-guiding line) and the effect of strain in the 10100 values as discussed in the text.

on the diffractometer used in those measurements, a small defect caused by chipping in one of the wafers was found in the 660 topograph. Note the increase in the apparent structure factor with increasing energy, in accordance with a corresponding increase in the universal strain parameter[4,45] p as χ_h decreases. The strained crystal is behaving, therefore, as expected; it is effectively a perfect crystal for long wavelengths and an imperfect one for short x-ray wavelengths. We may safely assume, however, that the influence of the strain at the lowest energy measured, Mo $K\bar{\alpha}$, is negligible. This is indicated by the good agreement of $F_{10\,10\,0(a)}$ with another independently measured value,[7] as well as the fact that the 10 10 0(a) value lies on a smooth monotonic curve passing through neighboring F_h's [see Fig. 7(b)]. In the absence of a well-tested theoretical treatment, we are unable to analyze the strain effect quantitatively. We should, however, point out that if we separate the structure amplitude into two contributions—a large one, taken as $F_{10\,10\,0(a)}$, from the unstrained crystal, and a small contribution ΔF of the strain—then $\Delta F^x = F_{10\,10\,0(x)} - F_{10\,10\,0(a)}$ $(x = b,c,d,e)$ is found to follow, rather closely, a power law in λ with an exponent of -3.

The conclusion emerging from the foregoing discussion is that the deviation in F_h is a real physical effect and does not have a hidden external cause. Let us assume then that the well-established Debye parameter $B = 0.4680$ Å^2 is valid for the entire range of $(\sin\theta)/\lambda$ explored in this study, and using f'_{CH}, let us calculate the "measured" atomic scattering amplitude f_m. A plot of the values thus obtained is given in Fig. 7(a) along with the theoretical relativistic Hartree-Fock f_{RHF} curve.[40] Figure 7(b) is a plot of the relativistic difference $\Delta f = (f_m - f_{\mathrm{RHF}})/f_{\mathrm{RHF}}$ versus $(\sin\theta)/\lambda$. The excellent agreement between theory and experiment for low $(\sin\theta)/\lambda$ and the smoothly increasing deviation as $(\sin\theta)/\lambda$ increases are clearly seen, as is the effect of strain in the 10 10 0 reflections.

Aldred and Hart[4] and Fehlmann[13] accounted for a slight decrease in the structure amplitude of the low-order planes by assuming an expansion of the valence shell. The data, analyzed on the basis of this assumption, yield a valence shell expansion of 6.8%. An attempt to account for the decrease in F_h in our case in a similar manner would require the inner shells to expand, since they contribute almost exclusively to the structure amplitude at high $(\sin\theta)/\lambda$. The expansion required can be calculated from

$$f_m[(\sin\theta)/\lambda] = f_{\mathrm{RHF}}\{(1+\epsilon')[(\sin\theta)/\lambda]\}\ ,$$

and yields $\epsilon' = 16\%$, 8%, and 6.2% for the 12 12 0, 999, and 10 10 0(a) data, respectively. While the possibility of an expansion of the inner shells cannot be completely ruled out, the systematic variation in the calculated values of ϵ', and especially their large magnitudes, which involve unreasonably high energy shifts for the levels involved, render such an explanation highly unlikely. A more fundamental approach along these lines, but starting with a monopole deformation term directly in the charge distribution of the Dawson theory (but not neglecting higher-order terms, as the core deformation can not be assumed *a priori* to be spherical), or even a modified set of the Doyle and Turner[46] wave functions used in calculating f_{RHF}, may, however, result in a better agreement with the experimental scattering amplitude for high $(\sin\theta)/\lambda$.

An alternative, and in our opinion a much better, way of accounting for the decrease in F_h at high $(\sin\theta)/\lambda$ is to assume that it originates in the Debye-Waller factor $\exp(-M)$ rather than the scattering amplitude. As mentioned earlier, $\exp(-M)$ is included both in $\epsilon = \epsilon_0 \exp(-M)$ and in F_H, which is proportional to $|f(k)|\exp(-M)$. Thus, the Debye-Waller factor determines both the period of the oscillatory structure in the rocking curve, Eq. (1b), through the cosine term, and the contrast. Since ϵ_0 is known,[27] these two items of information should, in principle, enable independent determinations of both the Debye-Waller factor and $f(k)$. In this experiment, however, the parameters chosen, namely t_1, t_2, λ, and the order of the measured planes, as well as the statistical accuracy of the data, rendered such a procedure unfavorable in terms of accuracy and computer time. Neglecting the very small corrections to $f(k)$, as well as the anharmonic temperature factor, the effective experimental Debye parameter B is the slope of the plot of

$$M = -\ln[(F_h/Q)_{\mathrm{meas}}/(f_{\mathrm{RHF}} + f')]$$

versus $(\sin\theta)/\lambda$, given in Fig. 8. It was found to be independent of the choice of the particular dispersion correction used. This figure demonstrates that both low-

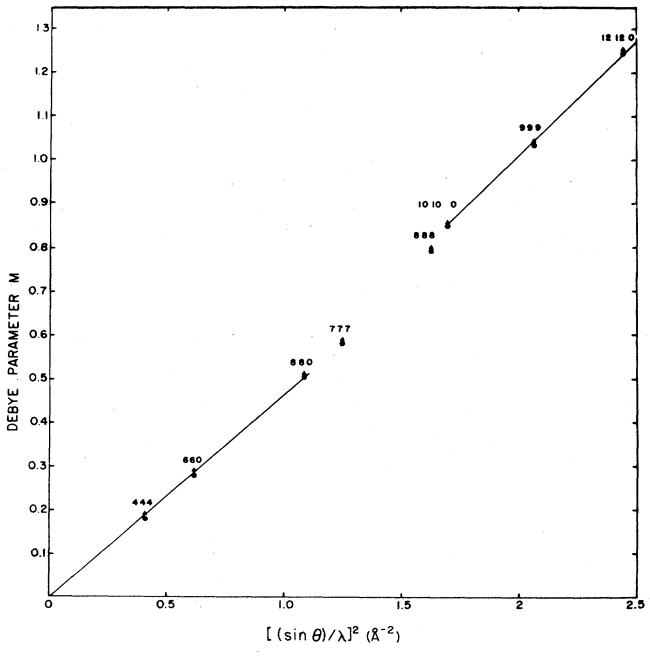

FIG. 8. Effective Debye-Waller parameter $M = -\ln[(F_h/Q)_{\mathrm{meas}}/(f_{\mathrm{RHF}} + f')]$ for $f' \equiv f'_{\mathrm{CH}}$ (dots) and $f' \equiv f'_{\mathrm{CL}}$ (triangles). Note the good fit to the straight-line sections at both ends of the plot. The Debye parameter $B = M[(\sin\theta)/\lambda]^{-2}$ corresponding to the slopes are $B_{\mathrm{low}} = (0.4632 \pm 0.0041)$ Å^2 and $B_{\mathrm{high}} = (0.5085 \pm 0.0035)$ Å^2. Note also that the dispersion correction does not influence the value of B; slopes are identical with both f'_{CH} and f'_{CL}.

and high-$(\sin\theta)/\lambda$ points lie on straight line sections through the origin, to a very good approximation. The slopes, and, consequently, the corresponding B, are, however, different at the ends of the $(\sin\theta)/\lambda$ interval.

Using the 440(b), 660, and 880(b) data, we obtain, for low $(\sin\theta)/\lambda$,

$$B_{\text{low}}=(0.4632\pm0.0041)\ \text{Å}^2\ ,$$

in very good agreement with the experimental values of (0.4613 ± 0.027) Å^2 of Aldred and Hart[4] and (0.4676 ± 0.0014) Å^2 of Price *et al.*[14] as well as the theoretical values of the valence-force-potential models[17,47] and the simple Born—von Kármán model.[48] B_{low} also agrees with the value of $B=(0.4671\pm0.0021)$ Å^2 that we calculated from F_h/Q values measured with Ag $K\bar{\alpha}$ radiation for the same reflections taken from the very recent data of Teworte and Bonse.[22] This seems to indicate that the Debye temperature of $\Theta_D=543$ K employed in that study, which corresponds to $B=0.444$ Å^2, is not even supported by their own data.

The three highest-order reflections, 12 12 0, 999, and 10 10 0(a), yield

$$B_{\text{high}}=(0.5085\pm0.0035)\ \text{Å}^2\ ,$$

which, while in very good agreement with the value of 0.5192 Å^2 predicted by the shell model,[16,17] is 10% higher than B_{low}. Since the contribution to the structure factor of the various electronic shells varies with the order of the Bragg reflection, a possible way of reconciling these two B values is by assuming different thermal-vibrational amplitudes in different parts of the bound atom. While all electrons contribute to the low-order Bragg reflections, the K electrons dominate the structure factor when $(\sin\theta)/\lambda>1.3$ Å^{-1}.

It has long been argued[49,5,6,17] that the bonding charges in the silicon crystal form a rather rigid structure whose thermal-vibrational amplitude is smaller than that of the silicon "cores." Since the Debye parameter B is proportional to the amplitude of the thermal vibrations, the corresponding Debye parameter B_{bond} will be smaller than B_{core}. Neutrons interact with the nucleus, which is assumed to move rigidly with the core electrons, while x rays interact with both the core and the bonding electrons. Combined neutron and x-ray measurements should therefore be able, in principle, to yield both B_{bond} and B_{core}. Moreover, B values obtained from neutron measurements, should be equal, or very nearly, to those obtained from high-$(\sin\theta)/\lambda$ x-ray measurements which probe the innermost electrons almost exclusively. Detailed analyses of temperature dependent x-ray and neutron measurements of the structure factor of the "forbidden" 222 reflection yield a bonding-electron Debye parameter ranging from[15] $B_{\text{bond}}=0.5B_{\text{core}}$ to[6] $B_{\text{bond}}=0.9B_{\text{core}}$. In all these studies it has invariably been assumed that the "cores," i.e., the nucleus and inner electrons move as a single rigid unit, and thus the two Debye parameters B_{bond} and B_{core} describe the thermal behavior of the atom in the crystal completely in that simple shell model. While this description is adequate for $(\sin\theta)/\lambda\leq1$ Å^{-1}, as the very good agreement between theory and experiment[4] shows, a modification of this approximation is introduced by our data for $(\sin\theta)/\lambda>1$ Å^{-1}. If the somewhat artificially sharp division of the atoms into bonding charges and "cores" is relaxed, and, rather than assuming only two different effective force constants, a smoothly and monotonously decreasing force constant is assumed to govern the motion of the various parts of the atom as one moves from the bonding charges towards the nucleus, then the thermal-vibrational amplitudes, and, consequently, the Debye parameter B, will increase correspondingly. The increase in the relative contribution of the inner shells of the atom to F_h upon increasing $(\sin\theta)/\lambda$ is accompanied by a corresponding increase in the effective Debye parameter. Over a limited range of $(\sin\theta)/\lambda$ values, the smoothly, but apparently slowly, varying B can be approximated by a constant effective Debye parameter. This is the reason for the different values obtained for B for $(\sin\theta)/\lambda\leq1$ Å^{-1} and $(\sin\theta)/\lambda>1.3$ Å^{-1}. A more quantitative analysis will have to await a theoretical formulation, as well as a larger body of accurate experimental F_h values, and, especially, a set of reliable dispersion corrections. We should only like to point out that the ratio

$$B_{\text{low}}/B_{\text{high}}=0.911\pm0.011$$

obtained here is suggestively close to the ratios

$$B_{\text{bond}}/B_{\text{core}}=\begin{cases}0.95\pm0.05, & \text{Ag } K\alpha_1\\ 0.85\pm0.05, & \text{Cu } K\alpha_1\end{cases}$$

obtained by Fujimoto[6] from "forbidden" F_{222} measurements. There is scope, therefore, for a rather detailed analysis of bound-atom vibration modes. Neutron scattering gives the nuclear motion. X-ray studies of low-order Bragg reflections give intermediate and mean electron vibrations, while the present high-order Bragg reflections can be used to determine the K-electron motions. X-ray and neutron studies of the 222 reflection yield the bonding electron Debye-Waller factor directly.

Another important conclusion, concerning the relative unimportance of anharmonicity in silicon, emerges from an examination of our data. Note that the sign of the leading anharmonic correction term in Eq. (8), i.e., f_cT_a, is given by c in Table II. As c is negative for 999 and positive for 777, we conclude, from Eq. (10) and the preceding discussion, that the anharmonic term in the effective one-particle potential should *increase* F_{777} by about 1% and *decrease* F_{999} by 2%. This should be manifested in Fig. 7(b), for example, as shifts of 1% downwards and 2% upwards for the 777 and 999 points, respectively, thus causing these two points to deviate significantly from a smooth curve passing through the rest of the data points. This effect is not observed. Using B_{low} and B_{high} for F_{777} and F_{999}, respectively, and their associated uncertainties, we obtain a limit on the magnitude of β which is about 3 times lower than that of Nunes.[36] This is in good agreement with the x-ray results of Aldred and Hart,[4] who lowered Nunes's limit by a factor of 2, but disagrees with the definite value of β measured using neutrons by Roberto *et al.*[5] In view, however, of the disagreement between different investigations of F_{222}, as discussed by Price *et al.*[14] and by Reid and Pirie,[17] as well as the uncertainty in the B value to be used

with high-order reflections, it is not clear that this indicates a significant underlying difference between neutron and x-ray results.

Finally, in view of the very low limit imposed by the data on β, the anharmonic term in the effective one-particle potential and the negligibly small static deformations obtained by the Dawson theory, for the reflections discussed here, it seems very reasonable to assume, as we have done, that the contributions of higher-order terms in the temperature factor, as well as possible static nonspherical contributions to the Debye-Waller factor B are also negligible to within the accuracy of our experiment. The dynamically deforming pseudoatom approach[50] conceptually agrees with the type of vibrational behavior indicated by our data. Unfortunately, an analysis of our data within the framework of this theory will have to await the availability of both a detailed theoretical treatment of crystalline silicon to high-$(\sin\theta)/\lambda$ values and a more complete body of high-order high-accuracy F_h values.

VI. CONCLUSION

We have presented here, for the first time, a set of measured structure factors F_h for high-order [$(\sin\theta)/\lambda > 1$ Å^{-1}] reflections in silicon with a thousandths-of-an-electron level of accuracy. The data complements and, at the lower end of the $(\sin\theta)/\lambda$ interval investigated, agrees excellently with the extensive low- and medium-order F_h data of Aldred and Hart.[4] At $(\sin\theta)/\lambda > 1.1$ Å^{-1}, systematic deviations from theoretical values based on a Debye parameter calculated from the low-order reflections are detected. This most probably indicates that the accepted view of regarding the silicon cores as rigidly moving has to be modified when high-order reflections, where the inner shells determine F_h almost exclusively, are considered. It is found that these reflections are better described by a Debye parameter about 10% higher than that of the medium-$(\sin\theta)/\lambda$ reflections.

In addition, no anharmonic contribution to the temperature factor in F_h is detected within the experimental accuracy. This lowers Nunes's[36] limit on β by a factor of 1.5 over the previous factor of 2 deduced by Aldred and Hart.[4] The contradiction of this conclusion and that of Roberto *et al.*[5] indicates the high desirability of additional high-accuracy and high-momentum-transfer F_h measurements.

ACKNOWLEDGMENTS

The hospitality of all members of the Physics Department, King's College, London, where this study was carried out, is gratefully acknowledged. We have greatly benefited from discussions with R. J. Weiss. One of us (M.D.) gratefully acknowledges the support of The Royal Society and The British Council.

*Permanent address: Department of Physics, Bar-Ilan University, Ramat-Gan 52100, Israel.

[1]H. Hattori, H. Kuriyama, T. Kateyawa, and N. Kato, J. Phys. Soc. Jpn. **20**, 1047 (1965); S. Kikuta, Phys. Status Solidi B **45**, 333 (1971); M. Hart and A. D. Milne, Acta Crystallogr. Sect. A **26**, 223 (1970); J. B. Roberto and B. W. Battermann, Phys. Rev. B **2**, 3220 (1970); M. Fehlmann and I. Fujimoto, J. Phys. Soc. Jpn. **38**, 208 (1975); R. W. Alkire and W. B. Yelon, J. Appl. Crystallogr. **14**, 362 (1981); R. W. Alkire, W. B. Yelon, and J. R. Schneider, Phys. Rev. B **26**, 3097 (1982).

[2]J. J. De Marco and R. J. Weiss, Phys. Rev. **137**, A1869 (1965).

[3]N. Kato and S. Tanemura, Phys. Rev. Lett. **19**, 22 (1967); S. Tanemura and N. Kato, Acta Crystallogr. Sect. A **28**, 69 (1972).

[4]P. J. E. Aldred and M. Hart, Proc. R. Soc. London, Ser. A **332**, 223 (1973); **332**, 239 (1973).

[5]J. B. Roberto, B. W. Batterman, and D. T. Keating, Phys. Rev. B **9**, 2590 (1974).

[6]I. Fujimoto, Phys. Rev. B **9**, 591 (1974).

[7]C. Cusatis, M. Hart, and D. P. Siddens, Acta Crystallogr. Sect. A **39**, 199 (1983).

[8]U. Bonse and R. Teworte, J. Appl. Crystallogr. **13**, 410 (1980).

[9]M. Deutsch and M. Hart, Acta Crystallogr. Sect. A (to be published).

[10]B. Dawson, Proc. R. Soc. London, Ser. A **298**, 255 (1967); **298**, 379 (1967); in *Advances in Structure Research by Diffraction Methods,* edited by W. Hoppe and R. Mason (Pergamon, London, 1975), Vol. 6.

[11]U. Pietsch, Phys. Status Solidi B **102**, 127 (1980); J. P. Walter and M. L. Cohen, Phys. Rev. B **4**, 1877 (1971).

[12]D. J. Stukel and R. N. Euwema, Phys. Rev. B **1**, 1635 (1970).

[13]M. Fehlmann, J. Phys. Soc. Jpn. **47**, 225 (1979).

[14]P. F. Price, E. N. Maslen, and S. L. Mair, Acta Crystallogr. Sect. A **34**, 183 (1978).

[15]J. R. Chelikowsky and M. L. Cohen, Phys. Rev. Lett. **33**, 1339 (1974).

[16]B. F. Robertson and J. S. Reid, Acta Crystallogr. Sect. A **35**, 785 (1979); W. Weber, Phys. Rev. B **15**, 4789 (1977); G. Nilson and G. Nelin, *ibid.* B **6**, 3777 (1972); W. J. L. Buyers, J. D. Pirie, and T. Smith, Phys. Rev. **165**, 999 (1968).

[17]J. S. Reid and J. D. Price, Acta Crystallogr. Sect. A **36**, 957 (1980).

[18]W. Kohn and L. J. Sham, Phys. Rev. A **140**, 1133 (1965); R. Gaspar, Acta Phys. Acad. Sci. Hung. **3**, 263 (1954).

[19]J. C. Slater, Phys. Rev. **81**, 385 (1951).

[20]N. Kato and A. R. Lang, Acta Crystallogr. **12**, 787 (1959); N. Kato, Z. Naturforsch. **15a**, 369 (1960); N. Kato, Acta Crystallogr. **14**, 526 (1961); **14**, 627 (1961); N. Kato, J. Appl. Phys. **39**, 2225 (1968).

[21]U. Bonse, W. Graeff, R. Teworte, and H. Rauch, Phys. Status Solidi A **43**, 487 (1977).

[22]R. Teworte and U. Bonse, Phys. Rev. B **29**, 2102 (1984).

[23]M. Lefeld-Sosnowska and C. Malgrange, Phys. Status Solidi **34**, 636 (1968).

[24]U. Bonse and W. Graeff, in *X-ray Optics,* edited by H. J. Queisser (Springer, Berlin, 1979).

[25]Z. G. Pinsker *Dynamical Scattering of X-rays in Crystals* (Springer, Berlin, 1978), Chap. 4.

[26]Routine E04FCF, NAG Subroutine Library, Mark 8 (Oxford, United Kingdom); P. E. Gill and W. Murray, SIAM J. Numer. Anal. **15**, 977 (1978).

[27]G. Hildebrandt, J. D. Stephenson, and H. Wagenfeld, Z. Na-

turforsch. **30a**, 697 (1975).
[28]*International Tables for X-ray Crystallography* (Kynoch, Birmingham, England, 1968), Vol. III, Chap. 3.2.2.
[29]G. Hildebrandt, J. D. Stephenson, and H. Wagenfeld, Z. Naturforsch **28a**, 588 (1973).
[30]D. P. Siddons, Ph.D. thesis, King's College, London, 1979.
[31]A. R. D. Rodrigues and D. P. Siddons, J. Phys. E **12**, 403 (1979).
[32]M. Hart and D. P. Siddons, Proc. R. Soc. London, Ser. A **376**, 465 (1981).
[33]F. C. Von der Lugt and H. A. Bethe, Phys. Rev. **71**, 612 (1947).
[34]B. Dawson and B. T. M. Willis, Proc. R. Soc. London, Ser. A **298**, 307 (1967).
[35]B. W. Batterman and D. R. Chipman, Phys. Rev. **127**, 690 (1962).
[36]A. C. Nunes, Acta Crystallogr. Sect. A **27**, 219 (1971).
[37]M. Abramowitz and I. A. Stegun *Handbook of Mathematical Functions* (Dover, New York, 1972), Chap. 10.
[38]See Ref. 37, Chap. 13.
[39]For example, Routine C235, Centre d'Etudes Recherche Nucleaires Subroutine Library (Geneva, Switzerland).
[40]*International Tables for X-ray Crystallography* (Kynoch, Birmingham, England, 1974), Vol. IV, Chap. 2.2.
[41]C. Cusatis and M. Hart, in *Anomalous Scattering,* edited by S. Ramaseshan and S. C. Abrahams (Munksgaard, Copenhagen, 1975).
[42]M. Deutsch and M. Hart, Phys. Rev. B **30**, 647 (1984).
[43]D. T. Cromer and D. Liberman, J. Chem. Phys. **53**, 1981 (1970); Acta Crystallogr. Sect. A **37**, 267 (1981); M. Hart and D. P. Siddons, in *Neutron Interferometry,* edited by U. Bonse and H. Rauch (Oxford University Press, Oxford, England, 1978).
[44]T. Takeda and N. Kato, Acta Crystallogr. Sect. A **34**, 43 (1978).
[45]M. Hart, Z. Phys. **189**, 269 (1966). N. Kato, J. Phys. Soc. Jpn. **19**, 971 (1964).
[46]P. A. Doyle and P. S. Turner, Acta Crystallogr. Sect. A **24**, 390 (1968).
[47]B. D. Singh and B. Dayal, Phys. Status Solidi **38**, 141 (1970); A. W. Solbrig, J. Phys. Chem. Solids **32**, 1761 (1971); R. Tubino, L. Piseri, and G. Zerbi, J. Chem. Phys. **56**, 1022 (1972).
[48]A. D. Zdetsis and C. S. Wang, Phys. Rev. B **19**, 2999 (1979).
[49]D. O. Welch, as reported in Ref. 5.
[50]N. H. March and S. W. Wilkins, Acta Crystallogr. Sect. A **34**, 19 (1978).